Dear Dr. Farinotti and Reviewers,

Thank you for your feedback on this manuscript. We have attempted to address all the points brought up in the reviews, this has resulted in several major changes to the modelling contained in the paper and thus the results and presentation. The following major changes were made:

1. As per the suggestion of Shawn Marshall and reviewer #1 we have changed the way the ETI model is distributed across the study area. Specifically, the residual temperature (representing melt processes other than shortwave radiation) is now kept constant across the grid. This is effectively the same as distributing the temperature based on equations 10 & 11 (described on P9). This has not substantially changed the results, but did resolve issues with poorly modelled melt on south aspects.
2. We have added an energy balance model and run four model formulations (both point and distributed models) for the month of July 2016 to compare the performance of the models against one another, and also against AWS data.
3. As per the suggestion of reviewer #2, we have revisited the methods for deriving albedo from orthoimages. Values are now scaled by fixing the value of the AWS cell to be the average measured between July 21-24, rather than assigning the average of July 13-31 as the upper end. This means that albedo in the AWS grid cell is constant throughout the model runs. We have tried to better explain our methods in text, and have also addressed the slight darkening between July 21 and 23.
4. During our revision of the models we discovered an indexing problem in the solar radiation model. Correcting this problem has dramatically improved the radiation values in the model.
5. The vast number of data points in UAV datasets make teasing out relationships difficult. We are constantly trying to improve the way we address this and have adopted a new strategy using robust statistical measures to calculate correlations. We acknowledge that both reviewers suggested adding figures showing the relationships between model error and aspect, slope, and water flow. The number of data points we are dealing with (>18 million) makes these type of figures unintelligible, so we have chosen to leave them out. Instead we have added a table of correlation statistics and a discussion of the difficulty of using traditional statistical measures in this study.

Below are our responses to the specific comments of the reviewers. Page and line numbers in our response refer to the track changes version of the document.

Thank you,
Eleanor Bash

Reviewer 1 comments:

(Page)1-(Line)1: While I think that all the necessary information is here, the first 5-6 sentences should be reworked to improve the flow from short, individual sentences. It currently reads like bullet points.
Done. P2-L1-7
2-8: Rework the sentence to reflect citations relevant to TI, ETI and EB, separately.
Done. P2-L16-17
2-12: Check sentence continuity.
Done. P2-L20
2-25: Typo
Done. P2-L35
2-35: NU? I assume Nunavut. Perhaps write out in full for the few instances for the benefit of the reader.
Done throughout.
3-10: Include the size of your study area: 0.185km2
Done. P3-L22
3-12: AWS melt I assume refers to a sonic depth gauge? Specify what you mean here. . . It is measured quantities that you refer to??
Clarified. P3-L25
3-17: Try to keep consistent with units. . . Here you move from metres when talking about error to cm for melt rates. These values are also surely in a water equivalent? This was a concern of mine when reading the manuscript as I was unsure if you are comparing UAV differencing (Z difference in m./cm.) and modelled melt (m w.e. /cm w.e.).
Units have been changed to be consistent throughout.
3-25: You describe your methodology for pole tilt of the SDG, but the dates of your ETI model (at both point and distributed) extend beyond the UAV measured differences with no real justification for why. . . perhaps I've missed something here or it hasn't been explained.
Clarified. P4-L8
3-30: "30" what??
Clarified. P5-L4
3-31: I'd like to see some reasoning for the selection of your chosen methodology for dealing with SDG data averages and gaps. Why the specified interval? Does it affect your results?
More description of methods has been added. P5-L4-11
4-4: Whilst this work is published in Bash et al. (2018) and doesn't all need to be repeated, I would like to see a few of the core details and justifications for methodologies of the SfM model construction. . . For example, why M3C2, and not 2.5d differencing was considered. A short reminder here would be useful.
Detail added. P5-L18-19
4-7: Is interpolation justified here? With what method? Why were their gaps in your DSM?
Detail added. P5-L20-21
6-7: So Iabs is SWnet? Perhaps change this terminology to be clear and consistent with the literature.
Changed throughout.

6-8: What are your derived TF and SRF values?! This is important to mention somewhere. Are your values believable? How do they compare to the other TI, ETI models (as you compare to in your discussion)?
A table of values has been added as well as a brief discussion of their relationship to other studies. P8-L27-P9-L2
6-9: I need some justification for modelling over these dates, and not just the DSM differencing period (3 days).
Clarified. P9-L4-6
6-11: Have some tests of the 0C threshold been performed? This threshold can be rather variable. I believe that optimising this threshold could be beneficial. This holds then to my major comment regarding the model. I believe the data and locality of the AWS makes it highly desirable to perform an energy balance approach for the pointscale, if not for both point and distributed models, to aid process understanding and support the application of your ETI approach. The authors have a lot of valuable data with which to calibrate/validate their model at the distributed scale (such as stakes and surface information from the UAV) with which to provide the best possible ETI model. Propagating the model error then with the DSM error can provide a strengthened analysis of how, in the best case scenario, the ETI succeeds/fails to capture important information about glacier mass loss.
Consideration of the implications of the threshold has been added. P8-L24-28
6-12: To distribute model variables. . . reword here.
This has changed substantially due to new model descriptions.
6-13: Although I agree that differences will likely be small, I think it valuable to distribute your temperatures in your model domain, as it may still vary enough to influence your 0C assumptions for melt onset. This also draws in to the limits of the residual approach you adopt, as mentioned in the open discussions by Professor Marshall. I think a simple environmental lapse rate would suffice for the small elevation range you describe.
See major revision comment 1.
6-15: This is modelled using the surface topography taken from the first DSM right? Specify that here.
Clarified. P7-L10
6-16: Another interesting and important aspect to test would be the effect of cell resolution. A 0.1 m resolution is incredible and interesting to test what models can and cannot do, but is not realistic for any level of glacier-scale or regional modelling. I think it relevant to have some level of testing, and discussion regarding this. For example, the ETI fails to capture the variability seen in the DSMs, but is this consistent at 1 m, 10 m, 30 m?
As per our previous response, we agree this would be a valuable analysis, but feel it would detract from the overall goal of the paper.
6-18: Provide minimum solar angles.
Done. P7-L15
6-26: Check sentence continuity.
Rewritten. P7-L26-28
6-27: Your figure 2 implies that you have a net radiometer (or rather both up-facing and down-facing pyranometers) to derive your albedo at the point-scale. How does this compare to your albedo map derived from your RGB histogram stretch from 0.55 upward? What are the ranges

of albedo derived? Also, the values seem largely different between 3 days when looking at figure 3. It looks as though the whole domain darkened by 0.05-0.1. Perhaps this was some effect of the cloud filtering you performed (according to Bash et al., 2018)?
A more detailed discussion of the albedo has been added. P8-L6-11
7-1: Still need some reasoning for your model period selection.
Clarified. P9-L14-16
7-10: Measured melt from the DSM? Again is this a Z-difference or ablation? Are you truly comparing the two here? I'm sure your model does not calculate vertical lowering, but melt (in w.e. units). Are you converting your DSM differences with density values of ice?? What values? Measured or assumed?
For consistency with SR50 measurements and M3C2 differences, the ETI model output is in m of surface lowering (since it is based on a statistical relationship with the SR50 measurement). The EB output is in m ice equivalent (not water). We have made the units more explicit in text.
7-11: Again, please provide some justification for NMAD and ME over other metrics.
A deeper discussion of statistics has been included. P9-Section 2.4
7-18: The model was run to quantify surface water production? Or just a 'watershed' analysis? Perhaps add a map of this to Figure 3?
Clarified. A map of this density and the linear potential accumulation features has been added in a new figure (Figure 6) P10-L15-21
8-9: The lower variability of the modelled values are not surprising, given that the model has two variables to consider for a system that is far more complex.
Agreed, however, the EB model shows the same patterns.
10-2: Figure 5A4-D4 does not show the correlation, but area of water features. I also fail to see how the errors of the AWS and distributed models are linked here. Perhaps include a correlation figure somewhere.
We have updated the final figure, which we hope makes it more useful to see the relationship between high error and W20m.
10-21: What uncertainties? Model uncertainties are not considered against your model-DSM comparisons. Your model error is simply the difference with the observed values.
We have expanded our discussion of uncertainty on P12-L2-10
10-22: Check citation format.
This sentence was removed.
10-27: what do you mean by muted?
Rewritten. P14-L7
10-32: Again, interested to see the effect of model resolution on your results as it would be very relevant for future work.
11-5: And Horizontal motion?
Added. P14-L20
11-12: Again to see another figure with some correlations would be nice.
11-17: Could this be a result of measurement uncertainty? Lighting from the processing of the SfM images? The processing of clouds and histogram stretching applied in your former paper? Although predominantly south facing, roughness may play a role here, which is of course not considered by ETI models.
After adjusting the model, this relationship has become negligible.

11-21: Have you considered any uncertainty due to SfM model construction for steep sided relic stream features that you mention? Did you obtain any oblique images? Is there anything worth noting about that here?

The streams within the study area are less than 1m deep. The larger deeply incised canyons are outside the study area.

12-16: Interesting that Figure 2 doesn't show such a dampened cycle. Please see suggestions for Figure 2. What about Wind speed? (again plot in Figure 2). . . A temperature factor will under-represent the contribution from turbulent fluxes if your glacier terminus is heavily affected by strong katabatic winds. Again, anything worth noting here?

This paragraph has been removed as suggested by reviewer 2.

13-3: The conclusion reads a bit like a discussion in places.

We have updated the conclusion with this in mind.

13-5: ETI 'model'. The albedo sentence feels a little out of place and should be reformulated into the previous sentence.

Done. P16-24

13-24: Add citations here.

This sentence was removed.

13-26: More pronounced compared to which studies?

See above.

[Figures]

Figure 2: Perhaps use colour here to aid the visual differences between measured and modelled point-based melt (or surface lowering??). For panel C. What do you mean by distributed variables? Surely the values are the same, as you are comparing the melt/surface lowering at the AWS? The variables require no distribution and surely are the same as panel B? Why not compare the measured and modelling SWin on the same panel to give confidence to the reader that your modelled radiation, based upon surface topography, is valid? Also, I would suggest converting units to Wm-2, for consistency with much of the literature, and to compare with other studies. As suggested in the specific comments above, I think it would be valuable to demonstrate the full EB data, including wind speed (and direction if there is anything interesting to say about katabatic winds and its directional consistency) as well as relative humidity and LW if available. Equally, showing the sub-period of the UAV DSM acquisitions is key!

Figure 2 has been updated to include color, and the other inputs of the energy balance model.

Figure 4: Your model error is Modelled minus Measured? So your negative values are under-estimation? Please clarify your convention. Transparent areas don't show where the model performs poorly, but rather where modelled-measured differences are within the error range of the measurements. What about model error estimates here? These should be propagated.

We have clarified our convention in text

Reviewer 2 comments:

1) There are several instances where the authors draw upon the methodologies of other studies to guide their ETI model development. However, what is often lacking is a simple description of the approach used in the cited study, and a statement explaining why this methodology was chosen by the authors. Examples of cited works that would benefit from deeper explanation include: Goswami et al. (2000); Bugler (1977); Rippin et al. (2015); Höhle and Höhle (2009)
We have added further detail to the methods used from these references P7, P10
2) A brief statement should be made early in the paper indicating whether reported melt values (m) are in ice equivalent or water equivalent (i.e. have you converted your surface elevation change observations to melt equivalent, or vice versa).
We have indicated the measurement units on P6-4, P8-L15
3) The determination of albedo is somewhat concerning, or at least the section describing the determination of albedo requires more detail and justification for the reader. It would be my impression that the scaling of surface albedo needs to be done twice, once for each orthoimage, with scaling being conducted using the albedo measured at the AWS at the time of the survey as validation for that cell. An off-ice site (rock or debris) could be used as a location of assumed constant albedo of ~0.1. Instead, it is unclear why the authors would use the AWS-derived average albedo (rather than maximum) as the upper limit for their albedo threshold across the area of interest on both survey days. Hopefully revisiting the albedo calculations might also help explain the surface darkening noticed by another commenter on the discussions page! Plotting the progression of surface albedo at the AWS over the study period could help confirm whether this darkening is real.
See comment above addressing changes to the albedo parameterization
4) A more detailed error analysis, and clearer reporting of errors and uncertainty, would significantly strengthen this work. Currently "model error" is used to describe the residual values between modelled (ETI_dist) and "measured" (see note below) melt at each cell. However, each of the parameters included in the model should have an associated (or at the very least estimated) uncertainty, as will the DSM models and calculated melt from DSM differencing.
We have expanded our discussion of the uncertainty. P10-L2
- To help with this, and to strengthen your argument for correlation between model errors and specific parameters, it could be worthwhile to include a figure with four plots that show model error vs. 1) aspect (with a full range from 0-360◦), 2) slope, 3) albedo, and 4) density of water features, by extracting these cell values over the entire region.
5) On a semantics note, the differencing of DSM models to determine melt is not a melt "measurement" but rather it is a calculation, or estimate (considering that the DSMs have their own model uncertainties). It is fair to treat the DSM melt estimates as a measurement for the sake of ETI model validation, but the authors should briefly acknowledge this and be clear about the source and magnitude uncertainties associated with this "measurement."
We have included more detail about the work of Bash et al. 2018. And explicitly acknowledged the assumption that melt and surface lowering are equivalent. P3-L29

6) One notable gap is an acknowledgement of, or discussion about, how parameters like aspect and slope are incorporated, or fail to be incorporated, into ETI_dist through the estimation of distributed radiation using the Goswami et al. (2000) approach. There is a good opportunity here to explore the sensitivity of ETI_dist to slope and aspect!

Specific/minor comments:

P1-L19: . . .14% of the world's glacier ice. . . ← specify if this is area or volume
Done. P2-L1
P2-L13: Available measurements. . . The wording of this sentence is awkward, rewrite or combine with previous sentence to help with clarity.
Rewritten. P2-L20
P2-L25: . . .in high temporal and spatial detail. . . (replace great)
Done. P3-L1
P3-L13-16: Regarding ablation stakes, I am curious why you did not also use these 17 ablation stake observations as validation for ETI_dist, in the same way you use the AWS as a point observation. Perhaps you did not have stake measurements on the days of the UAV survey. . . However, I am perplexed by the reporting of an RMSE for the stake observations, perhaps you mean the RMSE of the modelled melt (from DSM differencing) at the stake locations? It is important to be clear that your DSM differencing is not communicated "measured" melt, but rather modeled, or estimated, melt using the geodetic method.
We have tried to clarify the source of this reported uncertainty. P3-L26-29
P3-L23: Suggest including the manufacturers name for the SR50.
Done. P3-L25
P3-L31-32: Please provide some justification for why a 5-hour rolling average was chosen, and how samples qualified as being "significantly different" from the population.
We have added further description of this processing. P6-L1-11
P4-L3-4: When referring to resolutions (0.10 m, 0.02 m) specify whether these are horizontal resolution (your cell size) or vertical resolution; also be specific with the reported uncertainty – which is presumably vertical uncertainty? +/-?
Done. P6-L15-17
P6-L13: ". . .temperature was assumed to remain constant across the area." Out of curiosity, do you have a rough idea of what the temperature gradients are in this area? A quick correlation analysis between model error and surface elevations from your last DSM would be a simple way to verify that this assumption is reasonable.
The model now allows temperature to vary, see major revision comment 1.
P6-L15: What do you mean by "modify"? I would suggest giving much more attention to describing how the slope and aspect correction is applied in ETI_dist, particularly given the correlation of your error to aspect later on (see general comment #7)!
P6-L19-30: This is the section where it would be helpful to have some more detail from the previous studies you draw upon build your model and conduct corrections. This section really describes the heart of your model, and any additional detail you can provide will help readers understand the reasoning for your model design and why it performs the way it does. I might even suggest creating a simple flow-chart that illustrates the model inputs and their sources.

We have not included a flow chart, but have tried to expand on the description of both models.
P6-L27: Is there a reason your reported range in albedo goes from high to low? (Rather than "0.1-0.55"?)
New text here. P8-L29
P7-L12: As noted in the general comments, a brief explanation of the Höhle and Höhle paper's approach would be helpful – I am personally curious why the median is used instead of the mean!
A fuller description of the reasoning behind our choice of statistics has been added. P9-10
P7-L19: Why was 1500 cells chosen as the threshold for number of cells contributing to a water flow feature, and can you express this value in the area equivalent (e.g. square meters)?
Added. P10-L19
P8-L8: Uncertainties should be included the modelled and measured values reported here.
Added. P11-L14-17
P9-L4: Be clear what this correlation value is (Pearson correlation coefficient) or by using r = 0.34. Putting the correlation value at the end of this sentence seems awkward, maybe try rewording?
This section has changed. P12-13
P9-L7: Similar to above, correct to include ". . . much lower ($r < 0.1$, and $p >$ ___). . ."
See above.
P10-L1: Suggest observation rather than "experience" P10-L3: "-0.048 m"; also reword for clarity and include r =.
Done. P14-L13
P10-L15: ". . .deviation of 0.00083 m h-1, which is similar to other. . ."
This has been rewritten. P13-L25
P10-L20: Be specific, which year?
Rewritten for clarity. P14-L1
P10-L32: Specify, horizontal or vertical resolution
Done. P14-L12
P11-L4: "offsets"
Done. P14-L16
P11-L12: "Correlation between aspect. . ." This sentence feels out of place in a description of work by Bash et al. (2018), perhaps try rewording or open this paragraph with this sentence or something similar. E.g. "The correlation (r = X) between aspect and model error . . ."
This paragraph has been removed.
P11-L18: Tighten up wording, e.g. "Bash et al. (2018) measured higher melt rates in active supraglacial streams than on the surrounding ice."
Changed. P14-L31
P11-L23: ". . . between the density of linear. . ."
Rewritten. P15-L1
P12-L9-16: It is unclear what this paragraph contributes to the paper here, rather it seems to interrupt a discussion of water flow features and their impact on melt. Perhaps add more context, otherwise remove.
This has been removed.
P12-L20: ". . .have a greater relative importance."

This has been removed.

P12-L31: What do you mean by “simplifications”?

Clarified. P16-L15

P13-L5: Can you be specific about how you actually build upon the work of Rippin et al. (2015) to estimate albedo? Is this by introducing a scaling approach?

Reworded. P16-L24-25

P13-L10: Unclear what this first sentence is saying regarding “other implementations”

Clarified. P16-L29

P13-L19: It is not clear how Stevens et al. (2018) and the development of weather crusts relates to this study. Either take more time to explain the relevance (in the discussion section) or remove from conclusions.

More explanation has been added in the discussion.

Figure comments

Figure 2. Extending the E and F y-axis down to zero would help your arguments in the text. Check consistency with bold-type for your graph subsets and parenthesis e.g. A) vs (B), and correct formatting of Iin in the 2nd last line. Can you also explain the gap at the beginning of (F)?

Figure is substantially changed.

Figure 4. Recommend including the study dates – “. . . across the study area between July 21 (hh:mm) and July 23 (hh:mm).”

Done.

Assessing the performance of a distributed radiation-temperature melt model on an Arctic glacier using UAV data

Eleanor A. Bash[1] and Brian J. Moorman[1]

[1]Department of Geography, University of Calgary, Calgary, Alberta, Canada

Correspondence: Eleanor A. Bash (eleanor.bash@gmail.com)

Abstract. ~~Enhanced temperature index (ETI) models~~ Models of glacier surface melt are commonly used in studies of glacier mass balance and runoff, however, with limited data available most models are validated based on ablation stakes and data from automatic weather stations (AWS). The technological advances of unmanned aerial vehicles (UAVs) and structure-from-motion (SfM), have made it possible to measure glacier surface melt in detail over larger portions of a glacier. In this study, we use melt measured using SfM processing of UAV imagery to assess the performance of an ~~ETI~~ energy balance (EB) and enhanced temperature index (ETI) melt model in two-dimensions. Imagery collected over a portion of the ablation zone of Fountain Glacier, ~~NU~~Nunavut, on July 21, 23, and 24, 2016 was previously used to determine distributed surface melt. ~~Incoming~~ An AWS on the glacier provides some measured inputs for both models, as well as an additional check on model performance. Modelled incoming solar radiation and ~~temperature measured at the AWS, along with~~ albedo derived from UAV imagery, are also used as inputs for ~~the model which was~~ both models which were used to estimate melt from July 21-24, 2016. ~~Modelled melt agrees~~ Both models agree with melt measured at the AWS within ± 0.022 m (± 0.018 m for EB). Across the study area the median model error~~(-0.044 m)~~, calculated as the difference between ~~measured and modelled melt,~~ modelled and measured melt (EB$= -0.064$ m, ETI$= -0.050$ m), is within the uncertainty of the measurements. ~~A strong link was found between the model error and glacier surface aspect with higher errors linked to south aspects. The highest errors were also linked~~ The errors in both models were strongly correlated to the density of water flow features on the glacier surface. The relation between water flow and model error suggests that energy from surface water flow is contributing significantly to surface melt on Fountain Glacier. Deep surface streams with highly asymmetrical banks are observed on Fountain Glacier, but the processes leading to their formation are missing in the model assessed here. The failure of the model to capture flow-induced melt ~~and to under-estimate melt on south aspects~~would lead to significant underestimation of surface melt should the model be used to project future change.

1 Introduction

The Canadian Arctic Archipelago holds approximately 14% of the world's area of glacier ice outside the major ice sheets ~~(Gardner et al., 2011). Rates~~ and rates of glacier melt in the ~~Canadian Arctic~~ region have increased since the late 1990s ~~(Noël et al., 2018; Lenaerts et al., 2013; Gardner et al., 2012)~~(Gardner et al., 2011; Noël et al., 2018; Lenaerts et al., 2013; Gardner et al., . Fisher et al. (2012) show that recent melt rates on Canadian Arctic ice caps are the highest in 4000 years~~. Collectively,~~ , while Gardner et al. (2012) found that glaciers of the southern Canadian Arctic Archipelago contributed over 16% of 2003-2010 sea-level rise~~(Gardner et al., 2012)~~. Future projections indicate the glaciers from across Arctic Canada will continue to be the largest mountain glacier contributors to sea-level rise through the end of this century (Radić and Hock, 2011). Given the importance of Canadian Arctic glaciers to global sea-level rise and the rapid change in melt rates observed in recent years, it is critical to better understand the processes contributing to melt rates on these glaciers.

Direct measurements of melt rates on Arctic glaciers are scarce, only five glaciers from the Canadian Arctic have current data available online (WGMS, 2018). Where in situ data is collected, it is often based on ablation stake networks and data from automatic weather stations ~~(AWS) (e.g. Bash et al., 2018; WGMS, 2018)~~(AWS; e.g. Bash et al., 2018; WGMS, 2018). These in situ measurements must be extrapolated to provide estimates of melt at other locations on a glacier, or at other glaciers where no measurements exist. Several kinds of models are commonly used to extrapolate glacier surface melt measurements, including temperature index ~~(TI)~~(TI; e.g. Hock, 1999, 2005), enhanced temperature index ~~(ETI)~~(ETI; e.g. Irvine-Fynn et al., 2014; Bash and Marsha , and energy balance (EB; e.g. MacDougall and Flowers, 2011; Shaw et al., 2016). The TI or ETI models are often preferred for regional scale models, because of their lower computational needs and the ease with which input variables can be estimated. Energy balance models require more inputs and as a result are preferred for in depth studies of individual glaciers.

~~Validating model results is also difficult due to the lack of data available on Arctic glaciers~~ Lack of data for Arctic glaciers also makes it difficult to validate model results. Datasets are often split into training and validation periods to assess model performance~~. Available~~ , however, these measurements represent only a few locations on the glacier surface ~~, however~~ (Mair et al., 2003; Wake and Marshall, 2015; Matthews et al., 2015). Where outlet streams are measured, studies use total stream discharge and aggregated surface melt to validate results (e.g. Pellicciotti et al., 2005; Bash and Marshall, 2014). Validation with total melt provides insight into the average performance of these models over an entire glacier, but neither this method or the validation based on point data provide insight into model performance across a glacier surface.

Technological advances have allowed for increasingly detailed change detection from imagery obtained by satellites, unmanned aerial vehicles (UAVs), and terrestrial photography. Structure-from-motion (SfM) is widely used across a range of disciplines for reconstructing topography using imagery from the aforementioned sources (e.g. James and Robson, 2014; Cook, 2017; Watson et al., 2017; Lovitt et al., 2018; Bash et al., 2018). Employing SfM, Watson et al. (2017) use multiple reconstructions of a debris covered glacier to measure seasonal ice cliff retreat from terrestrial photographs, including spatial variation in rates across individual cliff faces. Using similar methods and UAV imagery, Bash et al. (2018) ~~measure~~ measured spatially variable melt rates in the ablation zone of an Arctic glacier over ~~3~~ 4 days. This new capacity for measuring change

in ~~great~~ high temporal and spatial detail provides opportunities to examine spatial patterns in ways that were previously not possible.

The methods of surveying that are needed for detailed surface change measurements using SfM are time consuming (Watson et al., 2017; Bash et al., 2018; Avanzi et al., 2018). These surveys involve multiple site visits, measurement of control points using differential GPS or total stations, and imagery collection (Bash et al., 2018). Given the effort involved in these data collection campaigns, it is not feasible at this time to extend these methods to regional-scale glacier change detection. Modelling efforts will continue to play an important role in understanding glacier melt in the future and thus it is critical to improve the models employed.

The aim of this study is to use melt measurements available in high spatial and temporal resolution to assess the performance of an ~~ETI model~~ energy balance model and an enhanced temperature index model across the glacier surface. We do this using previously published surface melt data which was measured using UAV surveys in the ablation zone of Fountain Glacier, ~~NU~~ Nunavut (Bash et al., 2018).

2 Methods

2.1 Study Area

Fountain Glacier, located on Bylot Island, ~~NU~~ Nunavut (Figure 1), has been studied in detail since 1991 (e.g. Moorman, 2003; Whitehead et al., 2014; Bash et al., 2018). The glacier stretches 16 km from higher elevations in the Byam Martin Mountain Range to its terminus roughly 10 km inland from the coast. The focus area of this study, in the lower ablation zone, spans a narrow elevation range (250–400 m) and terminates in a cliff face with two calving fronts. The lower portion of the glacier faces east, with several supraglacial streams of varying sizes (St. Germain and Moorman, 2016). The largest of these streams form deeply incised asymmetrical canyons, with a steeper north facing valley wall and a more gently sloping south facing valley wall (Figure 1).

During July of 2016 aerial surveys were conducted with a UAV to reconstruct ~~the~~ 0.185 km^2 of the glacier surface multiple times (Bash et al., 2018). Bash et al. (2018) measured surface lowering between July 21 and 24 using point cloud differencing across the study area indicated in Figure 1. Concurrently, an automatic weather station (AWS; Figure 1) ~~was recording surface melt~~ recorded surface melt with a Campbell Scientific SR50 sonic ranger, as well as temperature, incoming and outgoing shortwave radiation, relative humidity, wind speed and direction. Bash et al. (2018) assessed the surface lowering measured through point cloud differencing against 17 ablation stakes, as well as the AWS data, and found that the ~~surface lowering measured through point cloud differencing agreed with~~ measured surface lowering agreed with other melt measurements throughout the study area. In this study we assume that point cloud derived surface lowering is equivalent to surface melt. The uncertainty of this ~~The root mean square error (RMSE) of the measured~~ surface lowering was 0.048 m.

Bash et al. (2018) measured an average daily melt rate of ~~6.0 cm~~ 0.060 m day^{-1} across the study area between July 21-24, 2016. Average melt rates of ~~3.0–5.5 cm~~ 0.030–0.055 m day^{-1} were found by Whitehead et al. (2014) in summer ~~2010–2011.~~ 2010–2011. Bash et al. (2018) also showed, however, that melt was highly variable across the study area during that time

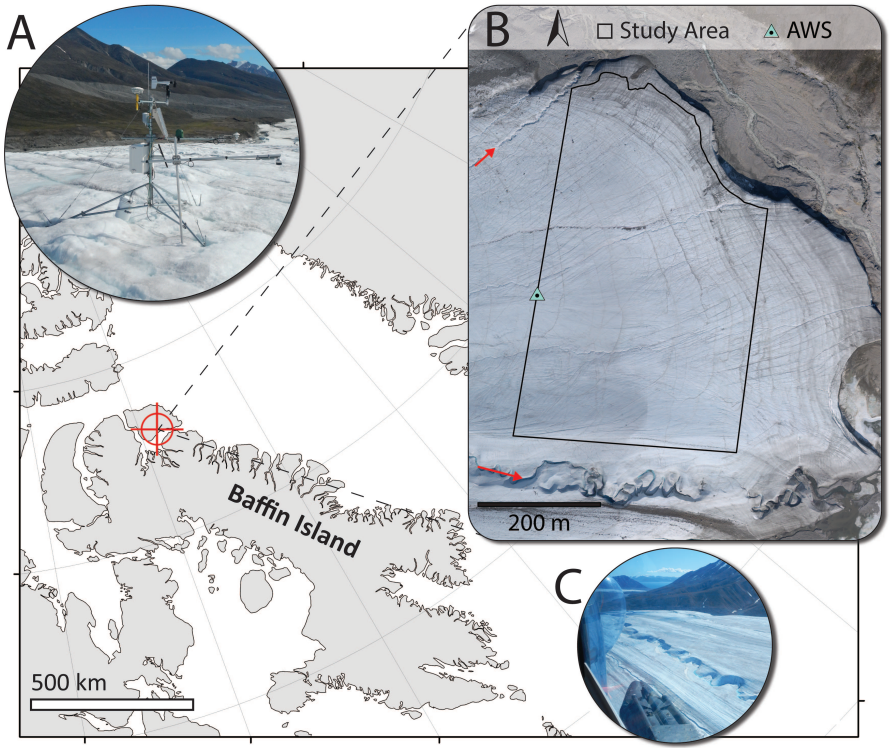

Figure 1. Location of Fountain Glacier on Bylot Island, ~~NU~~Nunavut, in the Canadian Arctic. (**A**) The automatic weather station (AWS) installed on a tripod, measuring incoming and outgoing shortwave radiation and temperature. An SR50 measuring surface position was installed on a separate pole drilled into the glacier (foreground). (**B**) A 2011 orthomosaic of the lower ablation zone of Fountain Glacier. The boundary of the study area is shown, the area extends to the 2016 glacier boundary on the north side. The AWS location is also indicated (green triangle). Two canyons formed by stream incision are indicated by red arrows. (**C**) An aerial view of the largest incised canyon on Fountain Glacier. The photo is taken facing east and the steep north facing canyon walls can be seen in contrast to the more gently sloping south facing walls.

ranging from ~~1.0–11.0 cm~~ 0.010–0.110 m day^{-1}. The authors found that these differences in melt were not tied to elevation or aspect of the glacier surface.

2.2 Description of Data

All AWS measurements were taken at 2 min intervals and recorded as hourly averages from July 13 to August 2, ~~2016 (Figure 2A, 2D, 2E). An~~ 2016 (Figure 2). The SR50 ~~sonic ranger~~ was installed on a pole drilled into the glacier surface immediately next to the AWS and measured hourly average surface position for the same time period. The pole holding the SR50 began to tilt due to melt out of the pole during the afternoon of July 27 and was reinstalled in the morning on July 28. The data from that time period was removed from the time series for model validation~~(Figure 2)~~.

Models run at high temporal resolution can have significant errors which stem from SR50 readings (Matthews et al., 2015). These errors stem from the uncertainty in SR50 readings due to the instrument accuracy (0.01 m), as well as uneven topography underneath the instrument. In addition to hourly surface position, the SR50 records a standard deviation of all measurements in the hourly average (typically 30 measurements). SR50 values where the standard deviation was greater than 0.01 m were removed~~and then~~, expected hourly melt rates are lower than the instrument accuracy and standard deviations greater than that are assumed to be related to noise. After removing those points, a 5 hr rolling average was calculated ~~.~~to smooth the data and fill in removed values. The 5 hr window was used to assure that all windows had multiple measurements to average, after some measurements had been removed. SR50 values which differed significantly from others in the 5 hr window were also removed (defined as more than the standard deviation of hourly change in the 5 hr window), under an assumption that it was physically unlikely for melt rates to change dramatically over short periods. Melt was then calculated in 12 hr periods (0:00 – 12:00) using the remaining values.

Processing of UAV imagery was done in Agisoft Photoscan and is described in detail by Bash et al. (2018). High accuracy settings were used to retain detail in the final point cloud. During processing, point clouds of the glacier surface at mid-day were produced for July 21 and 24, 2016. The point clouds were used to create orthomosaics and digital surface models (~~DSM~~DSMs) for each day with horizontal resolutions of 0.10 m.

The multiscale model to model cloud comparison algorithm (M3C2) was used to calculate melt across the study area at 0.02 m horizontal resolution (Lague et al., 2013; Bash et al., 2018), with vertical uncertainty of 0.048 m based on the RMSE of surface lowering compared to ablation stakes. The M3C2 algorithm calculates change normal to the local surface, which was desirable for measuring detailed change at such fine resolution. After differencing the point clouds were filtered to remove large outliers and differences calculated from fewer than 5 points, as suggested by Lague et al. (2013). This filtering resulted in variable density of points in the final point cloud. To align with DSMs and orthomsaics of the study area, for this study melt data was gridded to 0.10 m resolution. Melt measurements were averaged within each grid cell and empty cells were filled using bilinear interpolation.

2.3 Model Formulation

2.3.1 Energy Balance Model

An EB model accounts for all energy inputs and outputs at the glacier surface to estimate energy available for melt or freezing. As a representation of surface energy exchange, these models are often assumed to be the best estimators of surface melt (Hock, 2005). We employ an energy balance model described by Ebrahimi and Marshall (2016) as a check on both SfM-derived change and the ETI model described below.

$$Q_N = Q_{SW}^{\downarrow} - Q_{SW}^{\uparrow} + Q_L^{\downarrow} - Q_L^{\uparrow} + Q_H + Q_E \quad (1)$$

where Q_N is the net energy flux at the surface and $Q^{\downarrow}_{SW}, Q^{\uparrow}_{SW}, Q^{\downarrow}_{L}, Q^{\uparrow}_{L}, Q_H, Q_E$ represent incoming and outgoing shortwave radiation, incoming and outgoing longwave radiation, sensible and latent heat flux, respectively. The energy fluxes are all calculated in MJ for consistency with AWS measurements and energy fluxes are positive when they contribute energy to the glacier surface. When $Q_N > 0$ melt ($\hat{M}$; m ice) is calculated by:

$$\hat{M} = \frac{Q_N}{\rho_{ice} L_f} \tag{2}$$

where ρ_{ice} is the density of glacier ice, assumed to be 900 kg m^3 (e.g. Arnold et al., 2006; Cuffey and Paterson, 2010; Fitzpatrick et al., 201 and L_f is the latent heat of fusion. Longwave radiation (Q_L) is parameterized based on the absolute temperature (T) and emissivity (ε):

$$Q_L = \varepsilon \delta T^4 \tag{3}$$

where δ is the Stefan-Boltzmann constant. For $Q^{\uparrow}_{L}$, the calculation is straightforward if the surface is assumed to be melting (273.15 K), the surface emissivity is then 1.0. The atmospheric emissivity (ε_a) must be estimated in order to obtain $Q^{\downarrow}_{L}$. Here we use a parameterization from Ebrahimi and Marshall (2015) based on vapour pressure (e_v), and relative humidity (H), which was found to be robust when transferred directly without local training.

$$\varepsilon_a = 0.445 + 0.0055H + 0.0052e_v \tag{4}$$

The sensible and latent heat fluxes are calculated by equations 5 and 7, respectively.

$$Q_H = \rho_a c_p k^2 v \left[\frac{T_{pa} - T_{ps}}{ln(z/z_0) ln(z/z_{0H})} \right] \tag{5}$$

where ρ_a is the air density, calculated from the near surface air temperature and average air pressure at the AWS (P_{aws}=969), c_p is the heat capacity of air, v is the measured wind speed, and $k = 0.4$ is von Karman's constant. The potential temperature is calculated for the near surface air (T_{pa}) and ice surface by(T_{ps}):

$$T_p = T \frac{P_{ref}}{P_{aws}}^{R/c_p} \tag{6}$$

where P_{ref} is a reference pressure (1000 mb), $R = 288.5$ and the surface is assumed to be at the melting point.

$$Q_E = \rho_a L_v k^2 v \left[\frac{q_a - q_s}{ln(z/z_0) ln(z/z_{0E})} \right] \tag{7}$$

where L_v is the latent heat of vaporization, q_a is the specific humidity, based on T and H, and q_s is the specific humidity calculated from the saturation vapor pressure at the melting surface. z_0, z_{0H}, and z_{0E} are the roughness length scales for

turbulent exchange of momentum, heat, and moisture. The height of all AWS measurements is $z = 1.5$ m and $z_0 = 0.005$ m, was used as a tuning parameter at the AWS. Both equation 5 and 7 neglect a correction for atmospheric stability, which has been shown in previous studies to provide better results for these parameters (Hock and Holmgren, 2005; Ebrahimi and Marshall, 2016) .

A 1-D formulation of this model (EB_{aws}) runs using measured inputs from the AWS. A distributed version was also developed (EB_{dist}) using modelled incoming radiation at the AWS location and albedo derived from the UAV imagery to determine SW_{net} (both described below, Figures 2A, B, 3). Near surface air temperature across the study area was modelled using the uncorrelated AWS temperature and modelled radiation (Section 2.3.2). Measured values from the AWS are used for all other variables in equations 3 - 7. Distributed incoming radiation was ~~calculated~~ modelled by modifying the hourly measured incoming radiation at the AWS by the slope (S) and aspect (A) of each grid cell in the July 21 DSM (Figure 3C). The terrain correction was based on Goswami et al. (2000).

$$SW_{in} = Q^{\downarrow}_{SW} * cos\psi * cos(\omega - A) * sinS * cosS \quad (8)$$

where ψ is the solar altitude and ω the solar azimuth. This correction alone causes radiation to drop to zero overnight, which is not realistic during Arctic summers. Although direct radiation may drop to zero at some cells when sun angles are low overnight (solar elevation dips to 3.6°), diffuse radiation is at measurable levels (Figure 2E). A diffuse correction ~~was made~~ (SW_{diff}; based on Bugler (1977)~~to~~) was added to incoming radiation after correction for incidence angle to estimate the total incoming radiation (Figure 2F).

$$SW_{diff} = 16\psi^{0.5} - 0.4\psi \quad (9)$$

Lower peak radiation in the model (Figure 2B) is due to a slight difference in slope and aspect between the radiometer (which ~~is~~ was level) and the grid cell of the DSM containing the AWS (slope = 5°, aspect = 177°). Estimated radiation at each cell was then multiplied by $(1 - \alpha)$ to estimate ~~I_{abs}~~ SW_{net} at each cell.

Albedo was estimated across the study area using the orthomosaics from July 21 and July 23. Each orthomosaic contains the digital number recorded by the camera in the red, green, and blue (RGB) channels. The digital number cannot be directly used to calculate surface reflectance without conversion equations proprietary to the camera manufacturer. However, several studies have used other ~~means to convert digital numbers to surface reflectance (Corripio, 2004; Rippin et al., 2015; Ryan et al., 2017) , we employed an approach similar to that of Rippin et al. (2015)~~approaches to derive surface reflectance from digital numbers (Corripio, 2004; Rippin et al., 2015; Ryan et al., 2017). Rippin et al. (2015) use the sum of RGB digital number values as a proxy for albedo, similar to the approach we employ here.

Values for RGB channels were averaged and the total range scaled to ~~a range of 0.55-0.1~~ match the value at the AWS location (Figure 3). ~~The upper end of the range was determined by the average surface albedo measured at the AWS during the study period , while the lower end~~ Scaling in this way allows the values to be directly input into models, as opposed to providing a proxy for albedo as was done in Rippin et al. (2015). The average measured albedo value for the study period (0.31; July 21-24, 2016) was used to fix the rescaled value for both July 21 and July 23 at the AWS location. The lower end of the range

was based on albedo values of cryoconite holes reported by ~~Ryan et al. (2017). An~~ Ryan et al. (0.1; 2017), an assumption was made that cryoconite holes would have similar albedo to debris on the glacier surface. The scaling of RGB values was used to create ~~a gridded albedo product~~ two gridded albedo products that could be directly input into the melt model (Figure 3). July 21 albedo was used as a model input ~~for~~ up to 12:00 July ~~21 – 12:00 July~~ 23, while the July 23 albedo was used from 12:00 July 23 onward.

Mean albedo over the grid was 0.35 for July 21 and 0.33 for July 23, the median difference between the two was 0.020 (Figure 3). Albedo measured at the AWS on July 21 and July 23 at 12:00 (the time of image acquisition) was 0.315 and 0.309. The more pronounced difference in the gridded albedo likely reflects darker imagery in the July 23 mosaic, in addition to a true lowering of the surface albedo over the time period. To test the importance of this lower albedo value, total absorbed radiation at the AWS for July 2016 was adjusted to reflect a lower albedo, beyond what was measured at the AWS. This lowering of 0.014 could produce approximately 0.028 m additional melt over the course of the month.

2.3.2 Enhanced Temperature Index Model

This study assesses the performance of an enhanced temperature index model because these models are commonly used for regional scale estimations of glacier melt. The model we use is formulated after Bash and Marshall (2014), which uses absorbed radiation (SW_{net}; MJ hr^{-1}) and temperature (°C) in a linear regression model to estimate melt ($\hat{M}$; m ice). The formulation of the model is unique in that it controls for correlation between independent variables which can make model results unstable when not addressed. The uncorrelated temperature ($T_{residual}$) is calculated by:

$$T_{SW} = \eta + \beta SW_{net} \tag{10}$$

$$T_{residual} = T - T_{SW} \tag{11}$$

where η and β are coefficients fit using a linear regression. $T_{residual}$ is then used in the following equation to determine melt in meters of surface lowering consistent with SR50 and UAV measurements:

$$\hat{M} = \begin{cases} TF \cdot T_{residual} + RF \cdot SW_{net} & : T > T_T \\ 0 & : T \leq T_T \end{cases} \tag{12}$$

where SW_{net} can be calculated by the difference between incoming and outgoing radiation, or by multiplying incoming radiation by $(1-\alpha)$, where α is the surface albedo. The coefficients TF and RF were fit using a linear regression. Threshold temperatures (T_T) ranging from 1°- 2°C have been used in previous studies (Hock, 1999; Pellicciotti et al., 2005; Gabbi et al., 2014; Irvine- . Here we use $T_T = 0$°C. Although we have not performed any testing of this threshold, it is unlikely that it would affect model outcomes in this study as the air temperature rarely fell below 2°C during the month of July 2016, and never during the period where distributed melt information is available.

Table 1. Model coefficients obtained using linear regression modelling for July 14 – 20, 2016. Units of TF are mh^{-1}°C^{-1}, and RF are mh^{-1}MJ^{-1}

	TF	RF
This study	0.00019	0.0015
Irvine-Fynn et al. (2014) maximum	0.00068	0.0017
Irvine-Fynn et al. (2014) minimum	0.0002	-0.0014
Pellicciotti et al. (2005)	0.00005	0.0026

Cumulative positive $T_{residual}$ and SW_{net} were calculated for 12 hr periods beginning July 14 at 12:00. Data from July 14 – July 20 was used as a training period to determine the model coefficients (η, β, TF, RF) using a multiple linear regression. ~~The model will estimate no melt if actual air temperature falls below zero, but temperatures remained above zero through the study period.~~ The fitted model coefficients are shown in Table 1. Model coefficients compare well to those reported by Irvine-Fynn et al. (2014), a study which also modelled an Arctic glacier, although they report a wide range of values for RF depending on the training period.

A 1-D formulation of the model was run at the AWS site (ETI_{aws}) using measured SW_{net} and near surface air temperature. A distributed model (ETI_{dist}) was developed by estimating model variables across the study area at each grid cell. Given the relatively small size of the study area, $T_{residual}$ was assumed to remain constant across the area, calculated by equations 10 and 11 with modelled incoming radiation and measured temperature at the AWS site. Equations 10 and 11 can be used to back-calculate temperature when $T_{residual}$ and SW_{net} are known, this allowed modelled temperature to vary across the grid. SW_{net} was calculated from modelled distributed radiation and albedo, described above.

2.4 Model Performance

The four models (EB_{aws}, ETI_{aws}, EB_{dist}, ETI_{dist}) were run for the period 0:00 July 1–24:00 July 31, 2016, allowing for comparison between models over a longer time period than when melt measurements were available. Outputs from 0:00 July 14–24:00 July 31 were compared directly to melt measured with the SR50. To compare EB_{dist} and ETI_{dist} estimates, melt values were extracted from the grid cell containing the AWS. All models were assessed using the mean and standard deviation (σ) of the residuals ($\hat{M} - M$).

~~Melt~~ Total melt estimates for July 21–24 from ~~ETI_{dist}~~ both distributed models were compared to ~~measured melt~~ the gridded melt measurements across the study area for the same period. Model error was calculated at each grid cell in the study area, negative values indicate underestimation and positive values indicate overestimation of the model as compared to the UAV-derived data ($\hat{M} - M$). The median model error (ME) and normalized median absolute deviation (NMAD) were used to describe the model error following Höhle and Höhle (2009). Höhle and Höhle (2009) suggest using these metrics to describe errors when the error distributions are non-normal, which is typical for the large datasets produced with SfM (Montgomery and Runger, 2007). In the case of non-normal distributions, standard descriptive statistics (based on data means

and standard deviations) are disproportionately influenced by outliers, which the ME and NMAD are not (Maronna et al., 2006) . The median and range of measured and modelled melt were also calculated for comparison.

In addition to model performance, the model error across the study area was used to investigate factors influencing model performance. We examined model errors in relationship to surface characteristics which are known to influence the energy available for melt (Hock, 2005). ~~Correlations~~ The Pearson correlation coefficient is often used to assess variable relationships:

$$R = \frac{\sum_{i=1}^{n}(x_i - \bar{x})(y_i - \bar{y})}{\sigma_x \sigma_y} \tag{13}$$

where $\bar{x}$ and $\bar{y}$ are the variable means, σ_x and σ_y are the variable standard deviations. As noted above however, in the case that the mean and standard deviation are poor descriptors of a population, an alternative measure of relationship is necessary using robust estimators for the location and variance (Shevlyakov and Smirnov, 2011). Based on Shevlyakov and Smirnov (2011), we use the median correlation coefficient to assess the relationship between model error and potential explanatory variables.

$$R_r = \frac{\sum_{i=1}^{n}\frac{1}{n}(x_i - med(x))(y_i - med(y))}{NMAD_x NMAD_y} \tag{14}$$

In the case of large samples such as we have here (n>18 million), p-values are not a suitable measure for correlation significance (Maronna et al., 2006), instead we evaluate the strength of the correlation based on its value. Robust correlations were computed between model error and terrain variables (slope and aspect), albedo, and an estimate of surface water flow.

Water flow ~~was~~ direction and potential upstream catchment were quantified using the Hydrology Toolset in ArcGIS 10. Assuming that water is produced at every grid cell, flow paths were calculated from the July 21 DSM based on ~~up-slope~~ potential upstream accumulation. Cells with more than 1500 upstream cells were converted to a set of linear features and the number of these features within 20 m of each grid cell was calculated (W_{20m}). The ~~20 mradius was chosen to represent surface flowfeatures observed in the field~~1500 cell threshold represents 15 m^2 of upstream drainage area, and was chosen based on the assumption that 15 m^2 is likely to provide enough melt water to start flow. The resulting layer provided a representation of areas with significant surface water flow, including streams and thin sheet flows.

3 Results

3.1 Inter-model comparison at AWS

The four models were compared at the AWS site for July 1-31, 2016. All four models capture daily patterns of melt, with lower melt totals on average in the second half of the month, which is consistent with lower solar radiation recorded at the AWS (Figures 4A and 2B). The distributed models both consistently estimate lower melt totals than their point model counterparts, with differences more pronounced when melt values are high. This is most likely related to the lower shortwave radiation in

Table 2. Descriptive statistics for measured melt, modelled melt, and model residuals at the AWS site, July 14-31, 2016. All values were calculated based on 12-hr melt estimates and are reported in meters.

	Measured	EB_{aws}	ETI_{aws}	EB_{dist}	ETI_{dist}
Mean	0.022	0.022	0.023	0.019	0.021
σ	0.010	0.008	0.006	0.006	0.006
Total Residual		-0.016	-0.002	-0.064	-0.031
Mean Residual		0.000	0.000	-0.003	-0.001
Residual σ		0.009	0.011	0.009	0.010

the distributed model (Figure 2B). The EB models produce lower melt estimates than the ETI models when solar radiation is low. During periods of high incoming solar radiation, EB_{aws} and ETI_{aws} produce similar melt.

The total melt estimated during the month of July was lower in the two distributed models, $EB_{dist} = 1.223$ m and $ETI_{dist} = 1.394$ m, with standard deviation of 0.010 m , and RMS of 0.010 m. Performance of ETI_{dist} was similar, with a compared to the point models, $EB_{aws} = 1.436$ m and $ETI_{aws} = 1.508$ m. The EB models estimate less melt for the month than the ETI counterparts.

3.2 Model performance at AWS site

Model estimates from July 14-31, 2016 were compared to melt measured at the AWS site with the SR50. After tuning z_0, the mean residual of 12-hr melt estimates at the AWS was 0.000 m for EB_{aws} and -0.003 m for EB_{dist}. The fitted ETI_{aws} also had a mean residual of 0.000 m, while that of ETI_{dist} was -0.001 m. All four models underestimate melt at the site, with the distributed models underestimating more than the point models (Table 2; Figure 4B). The largest underestimate was from EB_{dist}. The variability of modelled melt is notably lower than measured melt in all cases.

3.3 Model performance over the study area

Across the study area median measured melt was 0.184 ± 0.048 m, the NMAD was 0.026 m (Figure 5B). Median melt across the area was lower in both EB_{dist} and ETI_{dist}, as was the variability (Figure 5A,C). The total range of measured melt was 0.305 m, while the range of $EB_{dist} = 0.123$ and $ETI_{dist} = 0.083$.

The ME ~~is lower than~~ and NMAD of $EB_{dist} = -0.064 \pm 0.022$, while that of $ETI_{dist} = -0.050 \pm 0.023$. The ME of ETI_{dist} is similar magnitude to the measurement uncertainty (0.048 m), indicating general agreement with measurements. When areas of error above the measurement uncertainty are highlighted (Figure 5D,E), ETI_{dist} shows clustered patterns representing ~~45~~53% of the total study area. Errors greater than twice the uncertainty (0.096 m) account for 5% of the study area. EB_{dist} errors greater than 0.048 m cover 79% of the study area, while those greater than 0.096 m cover 11%.

Model uncertainty can be derived from a number of metrics, including ~~the results of ETI_{AWS} and ETI_{dist}. Using statistical measures, model uncertainty is often quantified by the~~ variability in the ~~errors~~ model residuals, represented by the ~~RMS~~

Table 3. Robust correlation statistics (R_r) for surface characteristics and distributed models. Strong correlations are highlighted in bold.

	EB_{dist}	ETI_{dist}
Albedo	-0.207	-0.208
Aspect	0.177	0.178
Slope	0.204	0.197
W_{20m}	**0.470**	**0.462**

~~(0.011 m) and NMAD (0.026 m). However, in this case the 95th quantile of the errors (0.095 m) suggests this would be an underestimate~~NMAD or standard deviation. Based on assessment at the AWS site, uncertainty in 12-hr estimates from EB_{dist} and ETI_{dist} are 2σ = 0.018 m and 0.022 m, respectively. Bash and Marshall (2014) use validation at an AWS and incorporate uncertainties related to modelling input variables to estimate an uncertainty of 15%. In this study, we also have the benefit of examining distributed results across the study area through comparison with UAV derived melt. The variability of the distributed models is characterized by the NMAD, taking $2 * NMAD = 0.028$ m for EB_{dist} and $2 * NMAD = 0.044$ m for ETI_{dist}, these uncertainties are 4-6% of total estimated melt. Combined with the uncertainty in the measured surface change (0.048 m), a total uncertainty in the model errors can be derived ($\sqrt{2 * NMAD^2 + 0.048^2}$), $EB_{dist} = 0.056$ m, $ETI_{dist} = 0.065$. In either case, the errors which are strongly correlated with ~~surface aspect and~~ W_{20m} are higher than the combined uncertainty of measurement and model~~. These combined errors may range from 0.049–0.11 m.~~ , particularly for ETI_{dist}.

3.4 Relationship to surface characteristics

Moderate correlation was found between albedo, aspect, and slope for both EB_{dist} and ETI_{dist} (Table 3). Through field observation~~Through field experience~~, we were able to note a visual relationship between surface water features and high error during analysis (Figure 6A, C). This association was confirmed through correlation with W_{20m}, $R_r = 0.470$ for EB_{dist} and $R_r = 0.462$ for ETI_{dist}.~~A significant correlation (p<0.05) was found between model error and aspect, 0.34. Cells with south aspects had a mean error of -0.067 m, while those with north aspects had a mean error of -0.032 m. The relationship is visually apparent throughout the study area as well (Figure **??**A2-D2, A3-D3), and is particularly notable along east-flowing supraglacial streams (Figure **??**B2-3, D2-3). Statistically significant correlations were found with slope and albedo, but correlation values were much lower (<0.1), and thus were not investigated further.~~

~~Four example locations showing model error, surface aspect, and density of water features. Extents of example locations (**A–D**) are shown in the inset map. Panels show the orthomosaic (**1**), model error (**2**), aspect (**3**), and water feature density overlain by water features (**4**). The strong relationship between surface aspect and model error can be seen in all four locations. In A2 model error is low, despite high stream feature density, due to predominantly north aspect. While in **B1-3**, **C1-3**, and **D1-3** areas of high error are associated with predominantly south aspects and high density of water features. In **B2-3** and **D2-3** west-east flowing streams have high errors on south aspect banks, and generally lower or minimal error on north facing banks. Areas of positive model error (**A2**) are found where large boulders are present on the glacier surface.~~

Although most of the errors are negative, positive errors (i.e. overestimation) were also found. These are primarily associated with boulders and other large stationary objects on the glacier surface.

4 Discussion

Model results at the AWS indicate that both tuned point models perform very well. Performance of the distributed models is poorer, with EB_{dist} performing worse than ETI_{dist}, despite the physical basis of the energy balance model. This is likely due to a combination of factors, including limited data inputs available~~The ETI models derived using data from the AWS performed well during the validation period of July 21–August 2, 2016. Both ETI $_{AWS}$ and ETI_{dist} simulated melt at the location of the AWS to within 0.000±0.010 m per 12 hr period~~, and need for further refinement of energy exchange parameterizations. Previous work has shown that energy balance model performance is sensitive to variations in roughness length, wind speed, and albedo (Hock and Holmgren, 2005; MacDougall and Flowers, 2011) . Of these components, roughness length is the only EB model input used here that is not measured. An analysis of the model sensitivity to z_0 revealed a 10% decrease in total estimated melt (July 1-31) for $z_0 = 0.001$ m, compared to the reference run with the tuned z_0. Similarly, $z_0 = 0.01$ m resulted in a 7% increase in estimated melt. The deviation from the reference model run was caused by a 33% decrease and 22% increase in both Q_H and Q_E. Despite this sensitivity, $z_0 = 0.005$ provided the best fit for the training data.

Variability in both EB and ETI models is linked to solar radiation cycles. Despite the latitude of the study site, topography blocks direct solar radiation for a time during the night and causes strong diurnal variation in SW_{in}. The strength of that variation is much greater in the EB models than the ETI models (Figure 4A). As noted above, on clear sky days with relatively low temperatures, the EB and ETI models produce similar results (July 1-3). Under the opposite conditions, low SW_{in} and high temperatures (e.g. July 14-15, 28-29), the EB and ETI models produce the most dissimilar results. This is due to the relationship between temperature and radiation in the ETI model, where at low temperatures and high SW_{in}, $T_{residual}$ is very small and melt is driven primarily by radiation. At high temperatures and low SW_{in}, $T_{residual}$ is relatively larger and drives melt. In contrast, melt in the EB model is always primarily driven by solar radiation. Examining 12-hr averages of SW_{net}, LW_{net}, and $Q_h + Q_E$ in the EB model outputs, there is a strong correlation between SW_{net} and available melt energy ($R = 0.90$). The correlation between melt energy and LW_{net}, as well as $Q_h + Q_E$, is much lower ($R = 0.25$ and $R = -0.19$, respectively).

This contrast between the EB and ETI models, and the local tuning of the ETI model, allows ETI_{dist} to better estimate melt recorded at the AWS. For comparison to other studies, ~~this~~ σ residual from ETI_{dist} was converted to ~~a standard deviation of 0.00083~~ an hourly rate ($ETI_{dist} = 0.0005$ m h^{-1}~~. This performance~~), which is similar to other ETI models in the literature (Pellicciotti et al., 2005; Irvine-Fynn et al., 2014; Bash and Marshall, 2014). Irvine-Fynn et al. (2014) report a standard error of 0.00018 – 0.00053 m h^{-1}, the range in error stems from model runs with different training datasets. Hourly ETI model error reported by Pellicciotti et al. (2005) is as high as 0.0055 m water equivalent h^{-1}, compared to an energy balance model as reference data. Bash and Marshall (2014) report a standard error of 0.00031 m h^{-1}, when the ~~model is validated against data from a different year. While our results show a higher standard deviation, it is important to note that the uncertainties associated with modelling input data are likely to outweigh the discrepancies between this and other studies, as noted by~~

~~Bash and Marshall (2014); Pellicciotti et al. (2005).~~ ETI model is transferred in time. Overall these results at the AWS indicate that, in the absence of additional validation data, it would be reasonable to employ this model to estimate melt across the glacier surface.

Hock (1999) found that when TF is calculated based on melt and temperature records, it is highly variable. The inclusion of shortwave radiation in ETI models is an attempt to account for this variability. The low variability seen in the results of both $ETI_{~~AWS~~ aws}$ and ETI_{dist} when compared to AWS measurements is an indication of potential problems in the ETI models. Similar ~~muted model estimations were~~ variability was noted in other studies (Hock, 1999; Bash and Marshall, 2014). However, Hock (1999), Pellicciotti et al. (2005), and Irvine-Fynn et al. (2014), all cite R^2 values of 0.60, 0.86, and 0.80 when comparing total modelled melt to measured discharge. These previous results show that although the ETI models capture total melt, melt rates at individual points are captured less effectively. Similarly, we found across the study area that median modelled and measured melt agreed, but model results showed variability an order of magnitude lower than measurements (Figure 5~~A, B~~B, C). The availability of melt measurements at 10 cm horizontal resolution shed light on the areas where modelled and measured melt were (or were not) in agreement, which has not been shown before. These measurements also allowed us to examine possible explanations for the model errors, including the aspect and surface water flow.

It is worth noting that surface lowering measured through point cloud differencing is not always equivalent to surface melt. Vertical ice motion in the ablation zone ~~offset~~ offsets melt in measurements of surface change. However, in the case of Fountain Glacier Whitehead et al. (2014) estimate surface uplift to be 0.2 m over the course of the ablation season, or 0.002 m d^{-1}. Given the magnitude of measured surface elevation change over the 3 day period and the correspondence of those measurements to melt measured at ablation stakes, we assume that vertical uplift is a negligible contribution and the point cloud differences represent surface melt. Additionally, each point cloud was independently georeferenced each day, removing complications from horizontal flow.

~~The eastern orientation of Fountain Glacier results in primarily east draining supraglacial streams with north and south facing banks (Figure ??B, D). Bash et al. (2018) noted clear differences in measured melt on north and south facing stream banks, which was not seen in ETI_{dist} results. These differences in melt on opposite banks lead to the asymmetrical shape of canyons found on Fountain Glacier. Correlation between aspect and ETI_{dist} error was significant. South facing grid cells had an average error nearly twice that of north facing cells, with less variability in that error. Much of the study area is east and south facing, Figures ??B and ??D show east-west oriented streams with higher error on south facing banks. The northern portion of the study area slopes northward and overall has lower error (Figure 5C, Figure ??A). Close agreement between ETI_{AWS} and ETI_{dist} at the AWS, indicates the relation between model error and aspect is unlikely to be an artefact of radiation modelling. The explanation for the correlation remains unclear.~~

Bash et al. (2018) measured ~~melt rates within~~ higher melt rates in active supraglacial streams ~~higher than rates of melt on the ice surrounding those streams~~than on surrounding ice. This higher rate of melt leads to streams downcutting into the glacier surface over time, as long as melt water routing paths remain constant. Bash et al. (2018) also noted the difference in melt rate between an active stream and the nearby channel which the stream formerly occupied. During preliminary analysis of ~~ETI_{dist}~~ distributed model results, we ~~noted~~ observed the occurrence of high model errors in areas with visual evidence of

surface water flow including thin sheet flow and streams. Further investigation revealed correlation between model errors and the density of linear flow features (designated through DSM analysis and representing streams as well as thin sheet flow)~~and model errors less than -0.048 m, with a slightly more pronounced correlation on south facing aspects. Figure ??A is an example of an area with~~. The northern portion of the study area has predominantly north aspect, which exhibits high density ~~of surface water features~~in W_{20m}, but low model error. This pattern may result from lower melt on the north aspect, leading to less water production and flow than what is suggested by inferred flow paths in W_{20m}. The relation between model underestimation and surface water features suggests the water flowing on the glacier surface is contributing a measurable amount to surface melt. This is consistent with observed patterns of ~~down-cutting~~ downcutting streams and higher melt in active stream channels, but also shows the importance of water in areas with thin sheet flow over the glacier surface.

Stevens et al. (2018) note the role of kinetic energy in development of surface weathering crusts and the complexity of near-surface glacier hydrology which is only recently coming to light. Temperatures measured in a supraglacial stream on Fountain Glacier in 2014 ranged from 0-0.1°C (St. Germain and Moorman, 2016). These temperatures alone are not sufficient to explain the magnitude of model errors in the vicinity of water features, suggesting that other forms of energy transfer are playing an important role. Idealized crevasse bottom incision equations presented by Fountain and Walder (1998) are driven by discharge rates, suggesting a role in flow related incision for both heat advection as well as energy transfer from kinetic and potential energy. Irvine-Fynn et al. (2011) note that the relative importance of frictional heat contributing to incision rates in non-temperate glaciers remains unresolved. The results of this study suggest that further investigation into energy transfer (heat, kinetic, potential, frictional) from flowing water on non-temperate glaciers is necessary.

The ~~correlation~~ coincidence of high model error with water feature density was ~~significant~~ noted in areas with thin sheet flow, in addition to the locations of supraglacial streams. The contribution of melt energy to the glacier surface from less concentrated water flow found here has not been examined in previous studies, and these results add new insight to the emerging picture of complex surface hydrology on non-temperate glaciers, as suggested by Stevens et al. (2018). The ~~relatively lower correlation of model errors with water features on north aspects may be due to lower melt water production on north aspects, which leads to lower volumes of water flowing on north aspects of the glacier surface.~~

~~Daily melt rates on Fountain Glacier have been measured at 0.06-0.11 m d^{-1} (Whitehead et al., 2014; Bash et al., 2018). Similar melt rates have been measured on other glaciers in the Arctic (e.g. Arnold et al., 2006; ?), as well as mid-latitude glaciers (e.g. Bash and Marshall, 2014; Fitzpatrick et al., 2017). The ETI models are based on an assumption that solar radiation is the dominant component of glacier surface energy balance (Hock, 2005). Temperature then serves as a proxy for the remaining energy balance terms. Low solar elevations in Arctic summers result in total incoming radiation that is lower than that found at mid-latitude glaciers (Bash and Marshall, 2014; Fitzpatrick et al., 2017; Arnold et al., 2006; Bash et al., 2018). Although solar elevation varies over the course of the day in Arctic summer, 24 hours of daylight dampens diurnal variability in solar radiation as compared to mid-latitudes.~~

~~The~~ results of this study suggest that on Fountain Glacier the relative importance of energy flux from water flow is high enough to cause significant errors in the distributed model. ~~On Arctic glaciers, where overall melt rates are similar to mid-latitude glaciers, but solar radiation is relatively stable through the day, other energy contributions to the glacier surface may have more~~

relative importance. This has been noted in other studies (e.g. Hock and Holmgren, 2005), but ETI models continue to be employed for modelling glacier melt regardless of geographic context.

We believe that the relative importance of factors other than solar radiation which are driving melt on Fountain Glacier will have cumulative effects if ETI_{dist} or EB_{dist} were employed for long term modelling. Although this study looks at a short time frame of only 3 days, weather conditions during the study are similar to those found throughout the ablation season on Fountain Glacier and are likely to be representative of average conditions throughout the season. The high melt rates measured on south aspects and in areas of surface water flow, which are absent in the modelboth distributed models, are enough to change the terrain characteristics of the glacier over time (as seen in the formation of deeply incised canyons on Fountain Glacier). The changes in terrain feed back into melt dynamics related to slope and aspect. The inability of ETI_{dist} to capture higher melt seen on south aspects will fail to reproduce this canyon development, the inability of both models to capture the highest melt rates will slow these feedback mechanisms compared to observed evolution of the glacier surface (St Germain and Moorman, 2019) .

The availability of high resolution melt measurements now allows for analysis of model performance that is not possible with other methods of measuring melt (i.e. ablation stakes or satellite measurements). Building on previous studies of distributed energy balance models, high resolution distributed melt data may be used to develop more appropriate simplifications for glaciers similar to Fountain Glacier. Asymmetrical , which are more appropriate than primarily radiation driven models. Deeply incised canyons such as those found on Fountain Glacier have been noted on 83 other glaciers across the Arctic, including 10 on Bylot Island (St. Germain, 2019). Other studies of glacier terrain characteristics have found that gradual shifts in glacier aspect due to differential melt have important impacts on total glacier mass balance (Arnold et al., 1996, 2006). This reinforces the importance of developing a model which captures melt driven by both radiation and water flow.

5 Conclusions

We present the first study using high resolution measurements derived from SfM and UAV imagery to assess performance of a distributed ETI. In addition we build on the methods of Rippin et al. (2015) for estimating glacier surface albedo to derive a gridded albedo distributed energy balance and enhanced temperature index models, additionally we present a new method of deriving albedo from the UAV imagery that can be used directly in $ETI_{dist}$the grid-based model. The model developed in this study was compared directly to AWS measurements and to distributed measurements on a cell by cell basis. The availability of high resolution data revealed patterns in model performance that could not be found with other traditional methods of measuring glacier melt (i.e. ablation stakes or satellite measurements).

The ETI_{dist} exhibits similar performance at the AWS to other implementations of studies implementing ETI models. In the absence of high resolution distributed data, this model might be applied with confidence across the glacier surface. The bulk performance of the model across the study area is also similar to distributed melt measurements, with a median error lower than ME similar to the measurement uncertainty. However, the range in modelled melt melt from both models is an order of

magnitude lower than that seen in distributed melt measurements. The lower range in modelled melt combined with spatial patterns found in model error, allowed for investigation of sources of model error.

Significant correlation between surface water flow and model error highlighted the important role of water flow in melt dynamics on Fountain Glacier. Energy transfer from water flow in supraglacial streams is known to cause stream incision and was previously noted by Bash et al. (2018) on Fountain Glacier. The role of thin sheet flow on the glacier surface has not been studied previously, although Stevens et al. (2018) investigate near-surface hydrology and the role of kinetic energy in weather crust development. Our results corroborate the important role of kinetic energy in surface hydrology and suggest that on Fountain Glacier energy transfer from water flow is a significant driver of melt.

Given the importance of water flow in the development of deep canyons on Fountain Glacier~~and the absence of factors contributing to canyon formation in the ETI model~~, a model which accounts for water related energy inputs is necessary to effectively capture long term surface evolution on the glacier. ~~Other work has shown the influence of changes in surface slope and aspect on overall glacier mass balance, the relation found in this study between model error and aspect indicates the influence of aspect may be even more pronounced on Fountain Glacier.~~ A model which better reflects the drivers of melt on Fountain Glacier, and potentially similar glaciers across the Arctic, will provide insight into changing melt dynamics in these environments. In future work we hope to extend the time series of melt measurements from UAV imagery and use the distributed dataset to derive a new melt model which captures the melt drivers highlighted in this study.

Author contributions. The study was conceptualized by E.A.B., with supervision from B.J.M. Field data collection was designed and performed by E.A.B., with supervision from B.J.M. E.A.B. developed and implemented models, analysed all outputs, and prepared the manuscript. B.J.M. edited the manuscript and provided feedback on analysis.

Competing interests. The authors have no competing interests.

Acknowledgements. This work was supported by a Natural Sciences and Engineering Research Council Discovery Grant. Field support was provided by the Polar Continental Shelf Project, Parks Canada, Northern Scientific Training Program, and the Arctic Institute of North America. E. Bash was supported by the University of Calgary's Eyes High Recruitment Scholarship. We would like to thank Allison Gunther for fieldwork and technical assistance, and Mustafizur Rahman and Shawn Marshall for coding assistance. In addition, we would like to thank Shawn Marshall and two anonymous reviewers for valuable feedback on this manuscript.

References

Arnold, N. S., Willis, I. C., Sharp, M. J., Richard, K. S., and Lawson, W. J.: A distributed surface energy-balance model for a small valley glacier. I. Development and testing for Haut Glacier d'Arolla, Valais, Switzerland, Journal of Glaciology, 42, 77–89, 1996.

Arnold, N. S., Rees, W. G., Hodson, A. J., and Kohler, J.: Topographic controls on the surface energy balance of a high Arctic valley glacier, Journal of Geophysical Research: Earth Surface, 111, 2006.

Avanzi, F., Bianchi, A., Cina, A., De Michele, C., Maschio, P., Pagliari, D., Passoni, D., Pinto, L., Piras, M., and Rossi, L.: Centimetric accuracy in snow depth using unmanned aerial system photogrammetry and a multistation, Remote Sensing, 10, 765, 2018.

Bash, E., Moorman, B., and Gunther, A.: Detecting Short-Term Surface Melt on an Arctic Glacier Using UAV Surveys, Remote Sensing, 10, 1547, 2018.

Bash, E. A. and Marshall, S. J.: Estimation of glacial melt contribution to the Bow River, Alberta, Canada, using a radiation-temperature melt model, Annals of Glaciology, 55, 138–152, 2014.

Bugler, J.: The determination of hourly insolation on an inclined plane using a diffuse irradiance model based on hourly measured global horizontal insolation, Solar energy, 19, 477–491, 1977.

Cook, K. L.: An evaluation of the effectiveness of low-cost UAVs and structure from motion for geomorphic change detection, Geomorphology, 278, 195–208, 2017.

Corripio, J. G.: Snow surface albedo estimation using terrestrial photography, International Journal of Remote Sensing, 25, 5705–5729, 2004.

Cuffey, K. M. and Paterson, W. S. B.: Physics of Glaciers, Academic Press, 2010.

Ebrahimi, S. and Marshall, S. J.: Parameterization of incoming longwave radiation at glacier sites in the Canadian Rocky Mountains, Journal of Geophysical Research: Atmospheres, 120, 12 536–12 556, 2015.

Ebrahimi, S. and Marshall, S. J.: Surface energy balance sensitivity to meteorological variability on Haig Glacier, Canadian Rocky Mountains, The Cryosphere, 10, 2799–2819, 2016.

Fisher, D., Zheng, J., Burgess, D., Zdanowicz, C., Kinnard, C., Sharp, M. J., and Bourgeois, J.: Recent melt rates of Canadian arctic ice caps are the highest in four millennia, Global and Planetary Change, 85, 3–7, 2012.

Fitzpatrick, N., Radić, V., and Menounos, B.: Surface Energy Balance Closure and Turbulent Flux Parameterization on a Mid-Latitude Mountain Glacier, Purcell Mountains, Canada, Frontiers in Earth Science, 5, 67, 2017.

Fountain, A. G. and Walder, J. S.: Water flow through temperate glaciers, Reviews of Geophysics, 36, 299–328, 1998.

Gabbi, J., Carenzo, M., Pellicciotti, F., Bauder, A., and Funk, M.: A comparison of empirical and physically based glacier surface melt models for long-term simulations of glacier response, Journal of Glaciology, 60, 1140–1154, 2014.

Gardner, A., Moholdt, G., and Wouters, B.: Accelerated contributions of Canada's Baffin and Bylot Island glaciers to sea level rise over the past half century, The Cryosphere, 6, 1103–1125, 2012.

Gardner, A. S., Moholdt, G., Wouters, B., Wolken, G. J., Burgess, D. O., Sharp, M. J., Cogley, J. G., Braun, C., and Labine, C.: Sharply increased mass loss from glaciers and ice caps in the Canadian Arctic Archipelago, Nature, 473, 357–360, 2011.

Goswami, D. Y., Kreith, F., and Kreider, J. F.: Principles of solar engineering, CRC Press, 2000.

Hock, R.: A distributed temperature-index ice- and snowmelt model including potential direct solar radiation, Journal of Glaciology, 45, 101–111, 1999.

Hock, R.: Glacier melt: a review of processes and their modelling, Progress in Physical Geography, 29, 362–391, 2005.

Hock, R. and Holmgren, B.: A distributed surface energy-balance model for complex topography and its application to Storglaciären, Sweden, Journal of Glaciology, 51, 25–36, 2005.

Höhle, J. and Höhle, M.: Accuracy assessment of digital elevation models by means of robust statistical methods, ISPRS Journal of Photogrammetry and Remote Sensing, 64, 398–406, 2009.

Irvine-Fynn, T., Barrand, N., Porter, P., Hodson, A., and Murray, T.: Recent High-Arctic glacial sediment redistribution: A process perspective using airborne lidar, Geomorphology, 125, 27–39, 2011.

Irvine-Fynn, T. D., Hanna, E., Barrand, N., Porter, P., Kohler, J., and Hodson, A.: Examination of a physically based, high-resolution, distributed Arctic temperature-index melt model, on Midtre Lovénbreen, Svalbard, Hydrological Processes, 28, 134–149, 2014.

James, M. R. and Robson, S.: Sequential digital elevation models of active lava flows from ground-based stereo time-lapse imagery, ISPRS Journal of Photogrammetry and Remote Sensing, 97, 160–170, 2014.

Lague, D., Brodu, N., and Leroux, J.: Accurate 3D comparison of complex topography with terrestrial laser scanner: application to the Rangitikei canyon (N-Z), ISPRS Journal of Photogrammetry and Remote Sensing, 82, 10–26, 2013.

Lenaerts, J. T., van Angelen, J. H., van den Broeke, M. R., Gardner, A. S., Wouters, B., and van Meijgaard, E.: Irreversible mass loss of Canadian Arctic Archipelago glaciers, Geophysical Research Letters, 40, 870–874, 2013.

Lovitt, J., Rahman, M. M., Saraswati, S., McDermid, G. J., Strack, M., and Xu, B.: UAV Remote Sensing Can Reveal the Effects of Low-Impact Seismic Lines on Surface Morphology, Hydrology, and Methane (CH_4) Release in a Boreal Treed Bog, Journal of Geophysical Research: Biogeosciences, 123, 1117–1129, 2018.

MacDougall, A. H. and Flowers, G. E.: Spatial and temporal transferability of a distributed energy-balance glacier melt model, Journal of Climate, 24, 1480–1498, 2011.

Mair, D., Willis, I., Hubbard, B., Fischer, U., Nienow, P., and Hubbard, A.: Hydrological controls on patterns of surface, internal and basal velocities during three "spring events": Haut Glacier d'Arolla, Switzerland, Journal of Glaciology, 49, ~~555–567~~555–5671, 2003.

Maronna, R. A., Martin, R. D., Yohai, V. J., and Salibián-Barrera, M.: Robust statistics: theory and methods, John Wiley & Sons, 2006.

Matthews, T., Hodgkins, R., Wilby, R. L., Guðmundsson, S., Pálsson, F., Björnsson, H., and Carr, S.: Conditioning temperature-index model parameters on synoptic weather types for glacier melt simulations, Hydrological processes, 29, 1027–1045, 2015.

Montgomery, D. C. and Runger, G. C.: Applied statistics and probability for engineers, John Wiley & Sons, 2007.

Moorman, B. J.: Glacier-permafrost hydrology interactions, Bylot Island, Canada, in: Proceedings of the 8th International Conference on Permafrost, pp. 783–788, 2003.

Noël, B., van de Berg, W. J., Lhermitte, S., Wouters, B., Schaffer, N., and van den Broeke, M. R.: Six decades of glacial mass loss in the Canadian Arctic Archipelago, Journal of Geophysical Research: Earth Surface, 123, 1430–1449, 2018.

Pellicciotti, F., Brock, B., Strasser, U., Burlando, P., Funk, M., and Corripio, J.: An enhanced temperature-index glacier melt model including the shortwave radiation balance: development and testing for Haut Glacier d'Arolla, Switzerland, Journal of Glaciology, 51, 573–587, 2005.

Radić, V. and Hock, R.: Regionally differentiated contribution of mountain glaciers and ice caps to future sea-level rise, Nature Geoscience, 4, 91–94, 2011.

Rippin, D. M., Pomfret, A., and King, N.: High resolution mapping of supra-glacial drainage pathways reveals link between micro-channel drainage density, surface roughness and surface reflectance, Earth Surface Processes and Landforms, 40, 1279–1290, 2015.

Ryan, J. C., Hubbard, A., Box, J. E., Brough, S., Cameron, K., Cook, J. M., Cooper, M., Doyle, S. H., Edwards, A., Holt, T., Irvine-Fynn, T., Jones, C., Pitcher, L. H., Rennermalm, A. K., Smith, L. C., Stibal, M., and Snooke, N.: Derivation of High Spatial Resolution Albedo from UAV Digital Imagery: Application over the Greenland Ice Sheet, Frontiers in Earth Science, 5, 40, 2017.

Shaw, T. E., Brock, B. W., Fyffe, C. L., Pellicciotti, F., Rutter, N., and Diotri, F.: Air temperature distribution and energy-balance modelling of a debris-covered glacier, Journal of Glaciology, 62, 185–198, 2016.

Shevlyakov, G. and Smirnov, P.: Robust estimation of the correlation coefficient: An attempt of survey, Austrian Journal of Statistics, 40, 147–156, 2011.

St. Germain, S.: Studies of supraglacial canyons, personal Communication, 2019.

St. Germain, S. and Moorman, B.: The development of a pulsating supraglacial stream, Annals of Glaciology, 57, 31–38, 2016.

St Germain, S. L. and Moorman, B. J.: Long-term observations of supraglacial streams on an Arctic glacier, Journal of Glaciology, pp. 1–12, 2019.

Stevens, I. T., Irvine-Fynn, T. D., Porter, P. R., Cook, J. M., Edwards, A., Smart, M., Moorman, B. J., Hodson, A. J., and Mitchell, A. C.: Near-surface hydraulic conductivity of northern hemisphere glaciers, Hydrological Processes, 32, 850–865, 2018.

~~Thomson, L. I. and Copland, L.: Multi-decadal reduction in glacier velocities and mechanisms driving deceleration at polythermal White Glacier, Arctic Canada, Journal of Glaciology, 63, 450–463, 2017.~~

Wake, L. and Marshall, S.: Assessment of current methods of positive degree-day calculation using in situ observations from glaciated regions, Journal of Glaciology, 61, 329–344, 2015.

Watson, C. S., Quincey, D. J., Smith, M. W., Carrivick, J. L., Rowan, A. V., and James, M. R.: Quantifying ice cliff evolution with multi-temporal point clouds on the debris-covered Khumbu Glacier, Nepal, Journal of Glaciology, 63, 823–837, 2017.

WGMS, W.: Fluctuations of Glaciers Database, https://doi.org/10.5904/wgms-fog-2018-06, 2018.

Whitehead, K., Moorman, B., and Wainstein, P.: Measuring daily surface elevation and velocity variations across a polythermal arctic glacier using ground-based photogrammetry, Journal of Glaciology, 60, 1208–1220, 2014.

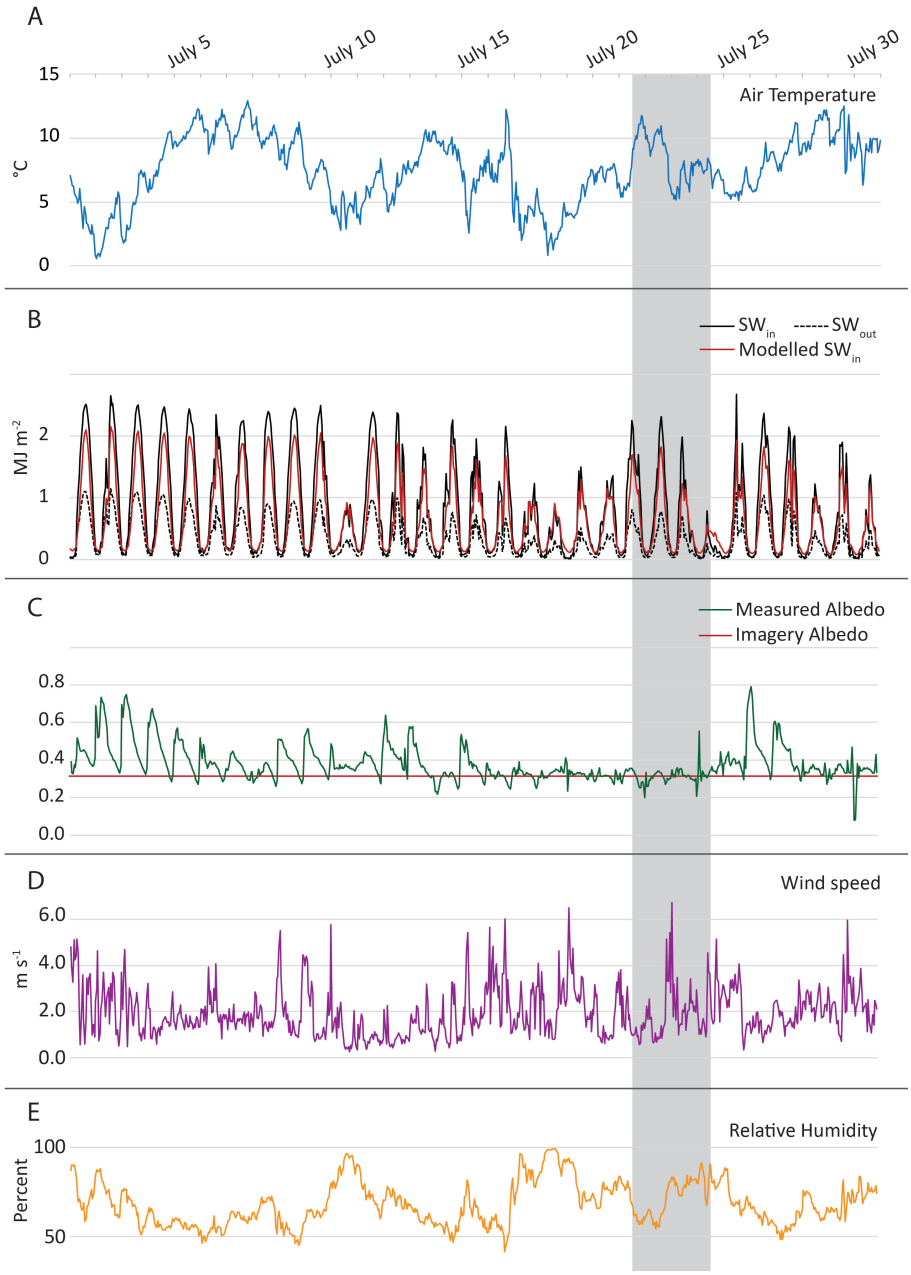

Figure 2. Hourly averaged melt model input variables, measured at the AWS for the period July 1-31, 2016. Variables include near surface air temperature (**A**), incoming (SW_{in}) and outgoing(SW_{out}) shortwave radiation (**B**), albedo (**C**), wind speed (**D**), and relative humidity (**E**). Inputs which are estimated for distributed models are shown in red, incoming shortwave radiation (**A**), and albedo (**B**). The albedo derived from UAV imagery is scaled using the average value at the AWS for July 21-24, so it remains constant throughout the model. The dates of the UAV study are shown in grey.

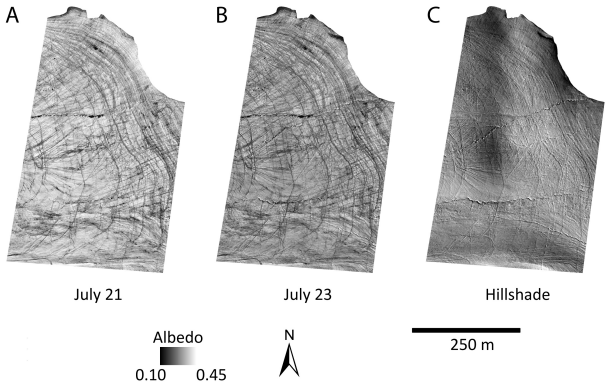

Figure 3. Albedo was derived from UAV imagery using an average values from RGB bands and scaling the lower and upper bounds to match the albedo of bare rocks (based on ~~REF~~Ryan et al. (2017)) and the average albedo measured on Fountain Glacier during the study period. (**A**) July 21 albedo values. (**B**) Juy 23 albedo values. (**C**) A hillshade model of the study area based on the DSM from July 21.

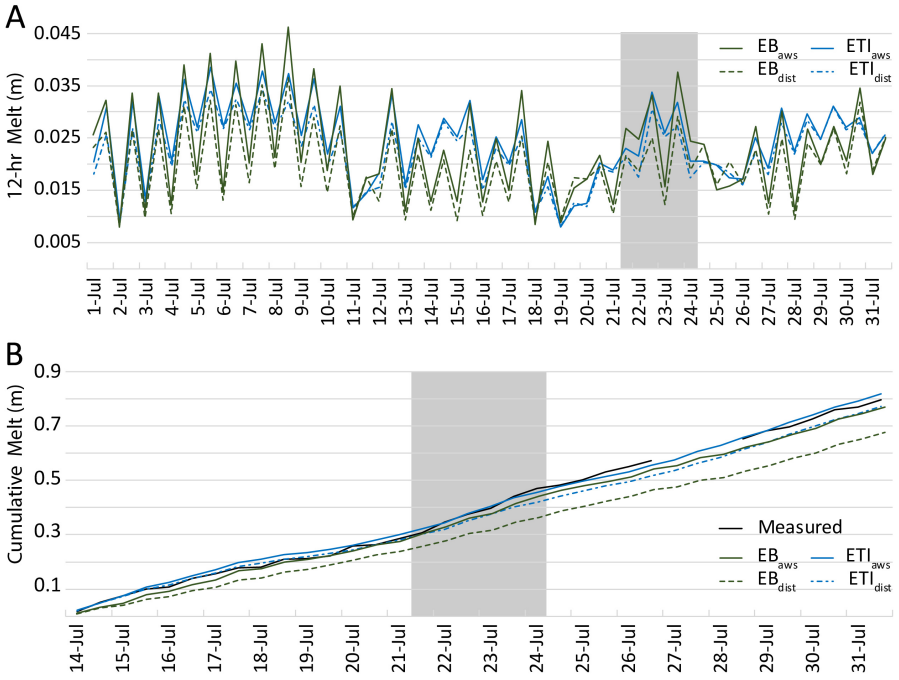

Figure 4. (**A**) Modelled 12-hr melt values at the AWS site, July 1-31, 2016. (**B**) Cumulative measured and modelled melt at the AWS, July 14-31, 2016. A gap exists in measured melt due to melt out of the pole holding the SR50. Melt was extrapolated during this time for better visual comparison, extrapolation was based on average melt rates for the day prior to and following the gap. The dates of the UAV study are shown in grey.

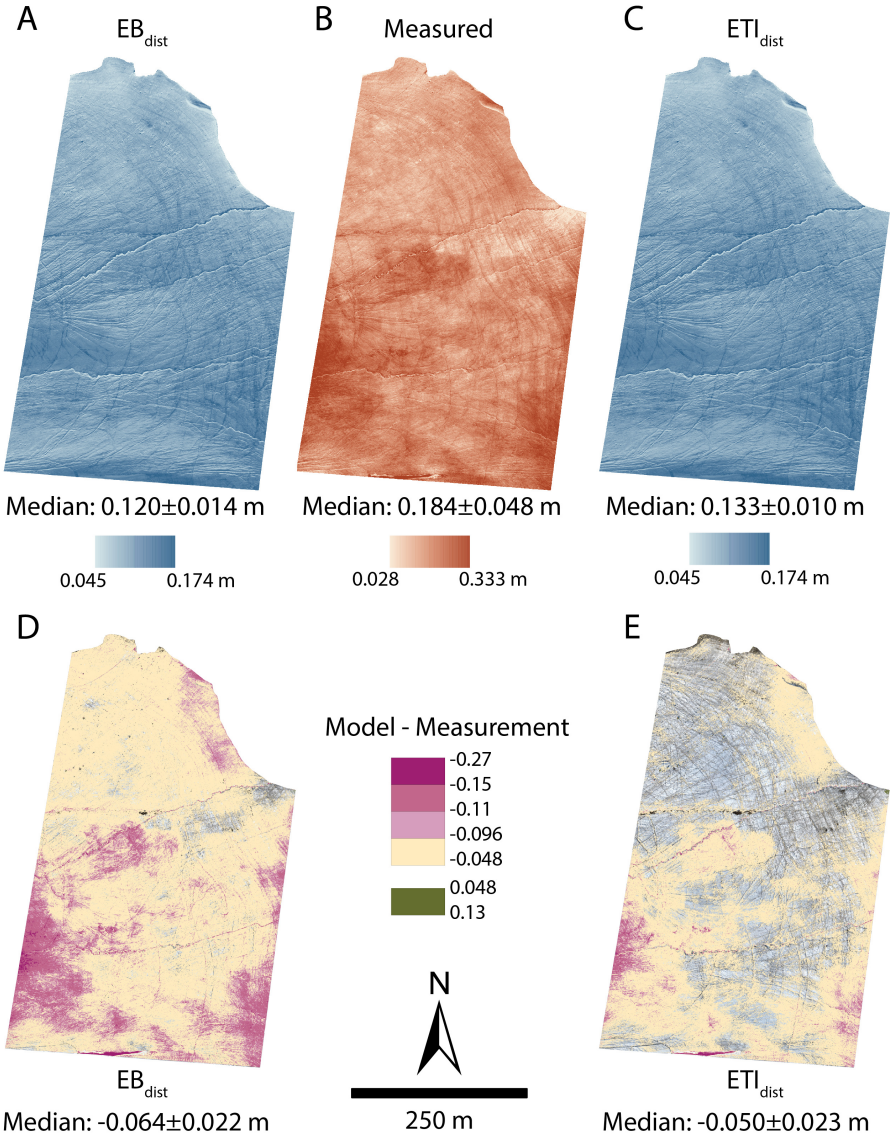

Figure 5. Distribution of measured and modelled melt across the study area between July 21 (12:00) and July 24 (12:00). (**A**) Melt estimated using EB_{dist} applied across the study area. (**B**) Melt measured through differencing surfaces reconstructed from UAV imagery. (**C**) Melt estimated using ETI_{dist} applied across the study area. (**D-E**) Model error, calculated by the difference between modelled and measured melt. Cells with an absolute value lower than the measurement uncertainty (0.048 m) are transparent to emphasize areas where the model residuals are high.

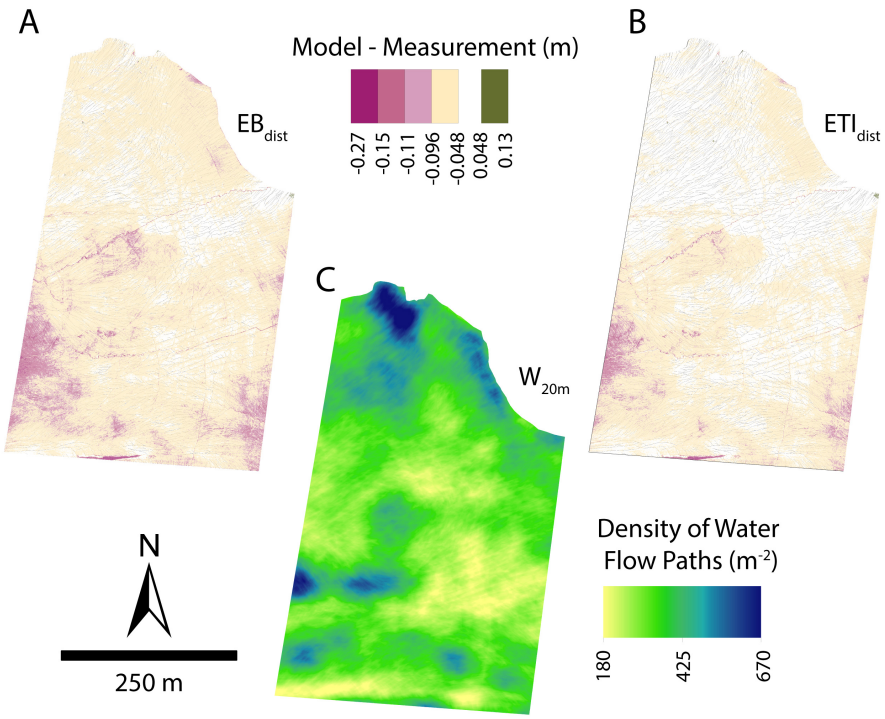

Figure 6. Model error with magnitude greater than 0.048 m underlain by flow path features with potential upstream accumulation greater than 15m^2 for (**A**) EB_{dist}, and (**B**) ETI_{dist}. Density of flow accumulation features within a 20 m radius of each cell (**C**).